ACS APPLIED MATERIALS & INTERFACES

Research Article

Cite This: ACS Appl. Mater. Interfaces 2019, 11, 3715−3721

www.acsami.org

An Enzyme-Free "ON-OFF" Electrochemiluminescence Biosensor for Ultrasensitive Detection of PML/RARα based on Target-Switched DNA Nanotweezer

Xintong Bian,[†,∥] Bin Guo,[†,∥] Min Zhao,[†] Daobin Han,[†] Wei Cheng,[‡] Fangzhou Song,[§] and Shijia Ding*[,†]

[†]Key Laboratory of Clinical Laboratory Diagnostics (Ministry of Education), College of Laboratory Medicine, Chongqing Medical University, Chongqing 400016, China

[‡]The Center for Clinical Molecular Medical Detection, The First Affiliated Hospital of Chongqing Medical University, Chongqing 400016, PR China

[§]Molecular Medicine and Cancer Research Center, Chongqing Medical University, Chongqing 400016, China

Supporting Information

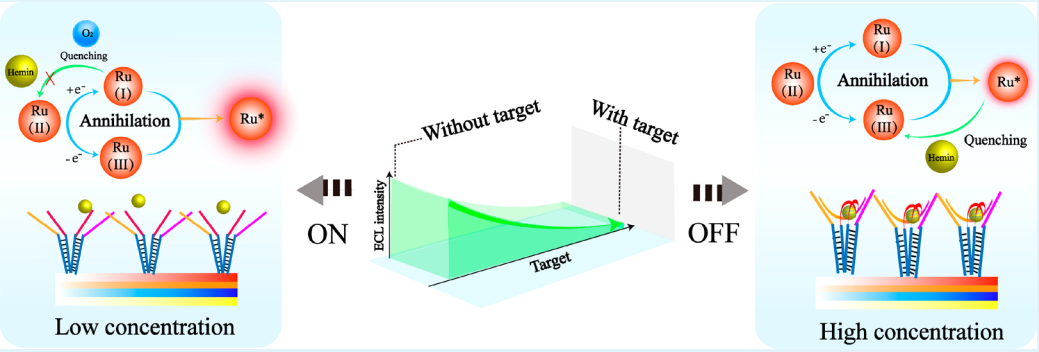

ABSTRACT: Herein, an enzyme-free "ON-OFF" electrochemiluminescence (ECL) biosensor for ultrasensitive detection of fusion gene PML/RARα is constructed based on a simple target-switched DNA nanotweezer as hemin concentration controller. In this biosensor, the hemin concentration is primarily controlled by the conversion of "opened-closed" DNA nanotweezers and low concentration hemin is first used as electrochemically regenerable enhancer. In the absence of the target, the nanotweezers are in an opened state which lead to a low concentration of hemin in the solution, resulting in an enhanced $Ru(bpy)_3^{2+}$ ECL signal. In the presence of the target, the closed nanotweezers absorbed onto the surface of electrode can capture the hemin, which achieves a high concentration of hemin and then quenches the ECL signal. The developed method achieves ultrasensitive detection of PML/RARα with a wide linear range from 1 fM to 1 nM and limit of detection as low as 0.125 fM. In addition, the ECL biosensor shows excellent specificity to the other subtypes of PML/RARα (subtype "S", "V"), "PML", and "RARα". Moreover, due to the high designable character of DNA nanotweezer, this method might provide a pragmatic $Ru(bpy)_3^{2+}$ ECL platform for ultrasensitive detection of nucleic acid in the future.

KEYWORDS: *electrochemiluminescence, hemin, DNA nanotweezer, enzyme-free, PML/RARα*

1. INTRODUCTION

With the development of nanotechnology, self-assembled DNA-based nanostructures, such as nanotweezer,[1] DNA box,[2] nanorobot,[3] DNA dendrimer,[4] DNA tetrahedron[5−7] and DNA hydrogel,[8] have been designed and widely applied in the field of biosensing, biological imaging and drug delivery. In variety of DNA nanostructures, DNA nanotweezers with excellent biocompatibility, good flexibility, and high programmability have shown great potential as signal transduction in biosensing construction.[1] Moreover, DNA nanotweezer is a flexible scaffold for use in the organization of molecules on the nanoscale, which can be engineered to site specifically incorporate functional elements in precise geometries' and to enable nanomechanical control capabilities. For example, Tan's group developed an integrated DNA tetrahedron nanotweezer (DTNT) as "ON-OFF" signal readout switch to reliably image tumor-related mRNA in living cells by fluorescence resonance energy transfer (FRET).[9] Later, our previous work designed a target-switched DNA nanotweezer to construct a sensitive logic gate chemiluminescent biosensor for microRNA detection.[10] Although the reported DNA nanotweezers are endowed with efficient signal nanoprobes, specific target

Received: October 23, 2018
Accepted: January 2, 2019
Published: January 4, 2019

DOI: 10.1021/acsami.8b18497
ACS Appl. Mater. Interfaces 2019, 11, 3715−3721

Scheme 1. Illustration of an Ultrasensitive "ON-OFF" ECL Biosensor for PML/RARα Detection Based on the Target-Switched DNA Nanotweezer As Hemin Concentration Controller

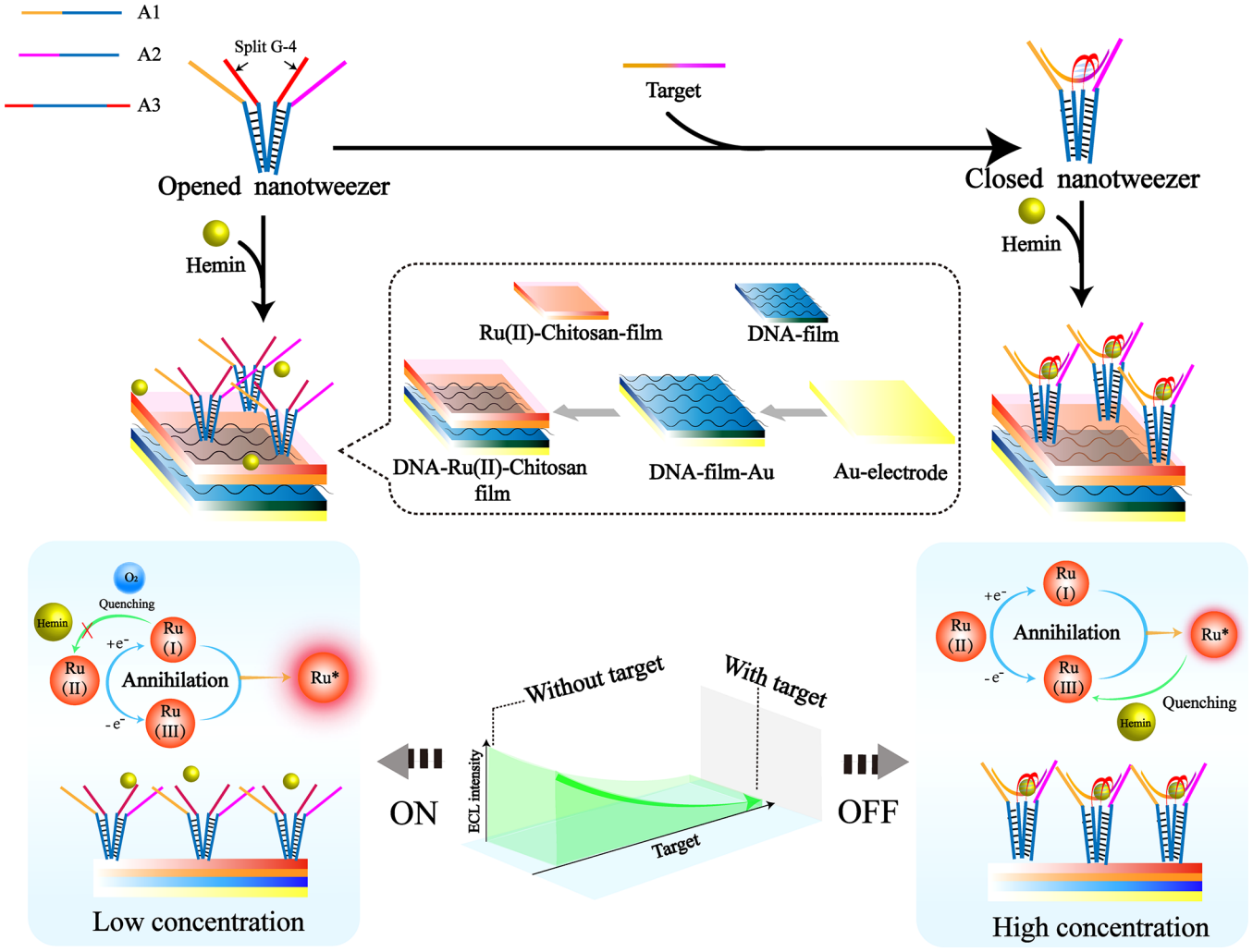

recognition and sensitive "closed-opened" switch, they still suffer from the drawbacks of the complicated self-assembly process, poor stability and low assembly efficiency. Hence, a highly efficient and simple DNA nanotweezer with different functions is urgently desired in the field of biosensing assay.

Electrochemiluminescence (ECL) is the luminescence resulting from the reaction between electrochemically generated positive and negative radical ions.[11−13] Ruthenium(II) tris(2,2′-bipyridyl) ($Ru(bpy)_3^{2+}$) is the widely used ECL luminophore due to its advantages of chemical stability, reversible electrochemical behavior and high luminescence efficiency.[14,15] Generally, the addition of efficient coreactants into $Ru(bpy)_3^{2+}$ aqueous solution is the common way to enhance the ECL signal.[16] However, it is reported that the dissolved oxygen (O_2) in $Ru(bpy)_3^{2+}$ solution can obviously quench the ECL signal, which limits the enhancement efficiency of coreactant.[17] Therefore, it remains challenge to develop a new strategy of enhancing ECL signal by reducing the quenching effect of dissolved oxygen. Hemin, an iron(III) porphyrin, can oxidize the excited state $Ru(bpy)_3^{2+*}$ to $Ru(bpy)_3^{3+}$ under a high concentration (0.38 μM), resulting in a significant ECL signal decrease based on the energy and electron transfer mechanism.[18] Interestingly, we found a phenomenon in pre-experiment: low concentration hemin (2 nM) can increase the ECL signal in $Ru(bpy)_3^{2+}$ aqueous solution. Furthermore, after deoxygenating toward the $Ru(bpy)_3^{2+}$ aqueous, low concentration hemin cannot enhance the ECL signal, indicating that low concentration hemin consumes the quencher O_2 for the indirectly enhancement of the $Ru(bpy)_3^{2+}$ ECL signal. Inspired by the found phenomenon, signal difference can be achieved by developing a target-triggered device to control the concentration of hemin. Here, a simple DNA nanotweezer with two split G-quadruplexes onto the top is designed to set as "ON-OFF" switching to control the concentration of hemin, which is further incorporated into the target-triggered proximity hybridization reaction for signal amplification.

As far as we know, the efficient immobilization of $Ru(bpy)_3^{2+}$ on the electrode can not only produce a high ECL signal, but also shorten the response time.[19,20] However, due to the instability character of pure $Ru(bpy)_3^{2+}$ modified on the electrode,[21] it is necessary to immobilize $Ru(bpy)_3^{2+}$ by employing some materials on the electrode for improving the stability.[22−24] Chitosan with excellent employability,[25] good biocompatibility[26] and positive charged character[27,28] can be polymerized with DNA film through the strong electrostatic interactions. The formed film on the electrode combines the excellent stabilization effect of chitosan with the high electron

DOI: 10.1021/acsami.8b18497
ACS Appl. Mater. Interfaces 2019, 11, 3715−3721

transfer efficiency of DNA film.[29] In addition, because of the positive charged character of chitosan, the designed DNA nanotweezers can be absorbed onto the film,[28] which adjusts the concentration of hemin.

PML/RARα (promyelocytic leukemia, retinoic acid receptor alpha) as an important biomarker of acute promyelocytic leukemia (APL), is of significance in leukemia diagnosis.[30,31] Herein, based on the target-switched DNA nanotweezer as hemin concentration controller, an ultrasensitive "ON-OFF" ECL biosensor is developed for PML/RARα detection. An overview of the designed ECL biosensing method is illustrated in Scheme 1. Initially, DNA−Ru(II)−Chitosan film is immobilized onto the working electrode surface. Hereafter, the DNA nanotweezer consists of A1, A2, and A3, among which the target recognition sites are set on the top of A1 and A2 and the split G-rich ends are set on the top of A3. Due to the effect of proximity hybridization, the "closed-opened" switch of DNA nanotweezer is controlled by the presence or absence of the specific target. Then, the formed DNA nanotweezers are attracted onto the surface of modified electrode by electrostatic interactions. In the absence of target, the split G-rich strands of DNA nanotweezers are away from each other (marked as opened nanotweezer), which cannot capture hemin dissolved in the $Ru(bpy)_3^{2+}$ solution. As a result, hemin is free in the solution and then further reacts with the quencher O_2, making ECL signal evident increase to obtain "ON" signal. On the contrary, in the presence of target, the recognition sites A1 and A2 bind with target, resulting in two split G-rich strands self-assembling into G-quadruplex for capturing hemin (marked as closed nanotweezer). Consequently, the ECL signal is quenched by high concentration of hemin on the electrode surface to obtain "OFF" signal. Thus, the "ON-OFF" ECL signal can directly reflect the target concentrations. More importantly, the proposed biosensing method exerts ultrasensitive detection of PML/RARα with one-step reaction based on the target-switched DNA nanotweezer, which possesses potential applications in the field of clinical analysis.

2. EXPERIMENTAL SECTION

2.1. Reagents and Materials. All the high-performance liquid chromatography (HPLC)-purified oligonucleotides (shown in SI Table S1) were synthesized by Sangon Inc. (Shanghai, China). The oligonucleotides were dissolved in hybridization buffer (pH 7.4, containing 30 mM sodium phosphate, 450 mM NaCl, 3 mM EDTA, 0.25% Triton 100), and stored at −20 °C. Ruthenium(II) tris(2,2′-bipyridyl) ($Ru(bpy)_3^{2+}$) and chitosan (Mw 113 kDa, degree of deacetylation 79.7%, low viscosity <200 mPa.s) brought from Sigma-Aldrich (St Louis, MO) were dissolved into deionized water and 1% acetic acid, respectively. Salmon sperm DNA (10 mg/mL) was purchased from Sangon Biotech. (Shanghai, China). Hemin was obtained from Sigma-Aldrich (St Louis, MO), and the diluted phosphate buffer solution (PBS, pH 7.4) contained 0.1 M K_2HPO_4, 0.1 M NaH_2PO_4, 0.1 M KCl, moreover, 0.1 nM HEPES and 1% dimethyl sulfoxide (DMSO) were also added for the better solubility. The PBS buffer was used in the whole process of ECL test. All other reagents were of analytical grade and without further purification. Deionized water from a Millipore water purification system (≥18 MΩ cm, Milli-Q, Millipore) was used in all experiments.

2.2. Apparatus. The ECL signal was executed with a model MPI-E ECL analyzer (Xi'an Remax Electronic Science & Technology Co. Ltd., Xi'an, China). The voltage of the photomultiplier tube (PMT) was set at 700 V, and the scanning range was from 0.5 to 1.25 V with the rate of 100 mV/s in the experiment. A conventional three-electrode system was used with a platinum wire as auxiliary electrode, Ag/AgCl as the reference electrode, and an Au electrode (Φ = 4 mm) as the working electrode during ECL detection. The structure of DNA−Ru(II)−Chitosan was confirmed by scanning electron microscopy (SEM, Hitachi, Tokyo, Japan) at an acceleration voltage of 25−30 kV. DYY-6C electrophoresis analyzer (Liuyi Instrument Company, China) and Biorad ChemDoc XRS (Bio-Rad, USA) were used for gel electrophoresis and imaging, respectively.

2.3. Preparation Process of Au Electrode Modified by DNA−Ru(II)−Chitosan Film. Chitosan (500 mg) was dissolved in 90 mL of 1% acetic acid. NaOH solution (0.2 M) and distilled water were added gradually into the solution to 100 mL (pH 5.0). 50 mg/mL $Ru(bpy)_3^{2+}$ solution was added into the above chitosan solution. After mixing up, the mixture was stored in the 4 °C refrigerator before use.

The Au electrode with 4 mm in diameter was treated with alumina slurry (0.3 and 0.05 μm Al_2O_3) to obtain a mirror smoothness, followed by sonication in ultrapure water for 5 min. The well-polished electrode was modified by DNA film through dropping 10 μL of DNA (10 mg/mL) solution onto the surface, and then dried at 4 °C for 8 h. Furthermore, 10 μL prepared Ru(II)−Chitosan solution was dropped onto the DNA film to construct the DNA−Ru(II)−Chitosan film and kept for 45 min in 37 °C. The modified electrode was stored in the refrigerator at 4 °C until used.

2.4. Preparation of DNA Nanotweezers. The 10 μL of 10 μM three DNA strands (A1, A2, and A3) were respectively added into an eppendorf (EP) tube with 10 μL hybridization buffer. Then, the mixture was incubated at 95 °C for 5 min and then gradually annealed to room temperature to form the desired opened DNA nanotweezer. The prepared opened DNA nanotweezers were both added into 5 mL PBS solution (400 pM of final concentration of each strand) and stored at 4 °C until used.

2.5. Gel Electrophoresis Analysis. The product solution was subjected to electrophoresis analysis on the 2% agarose gel electrophoresis (AGE). Electrophoresis was carried out in 1 × TBE buffer (89 mM Tris-boric acid, 2 mM EDTA, pH 8.3) at a 120 V constant voltage for 45 min. After that, the gel was visualized via gel image system.

2.6. Detection Protocol. Before the testing, different concentrations of target were added and incubated in a 50 μL mixture containing 20 nM opened nanotweezer at 4 °C for 8 h. Afterward hemin (2 nM) was added into the mixture and incubated at 37 °C for another 45 min to form closed nanotweezer. ECL measurements were conducted in a beaker (10 mL) that included 50 μL of the closed nanotweezer solution and 5 mL of the PBS solution. Afterward, DNA−Ru(II)−Chitosan modified Au electrode was inserted into mixture. Then, MPI-E ECL analyzer was used in the voltage range from 0.5 to 1.25 V with 100 mV/s and the voltage of the photomultiplier tube (PMT) was set at 700 V.

3. RESULTS AND DISCUSSION

3.1. The Influence of Hemin Concentration on $Ru(bpy)_3^{2+}$ Based ECL System. In $Ru(bpy)_3^{2+}$ based ECL

DOI: 10.1021/acsami.8b18497
ACS Appl. Mater. Interfaces 2019, 11, 3715−3721

system, the enhancement effect of low concentration hemin was surprisingly observed. For the further study of the mechanism, six-group control experiment was designed (shown in Figure 1): the ECL signal in $Ru(bpy)_3^{2+}$ solution

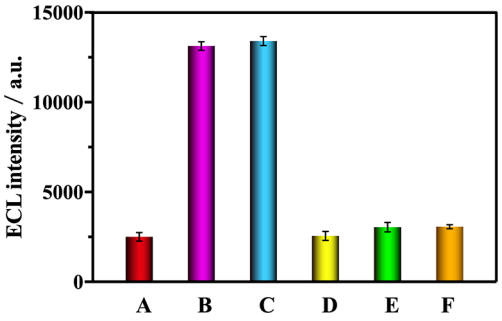

Figure 1. ECL signal of 6 control groups in different condition: ECL signal in $Ru(bpy)_3^{2+}$ solution (A); ECL signal in $Ru(bpy)_3^{2+}$ solution after deoxygenating (B); ECL signal in $Ru(bpy)_3^{2+}$ solution with hemin (C); ECL signal in $Ru(bpy)_3^{2+}$ solution added with hemin after deoxygenating (D); ECL signal in $Ru(bpy)_3^{2+}$ solution added with hemin before deoxygenating (E); ECL signal in $Ru(bpy)_3^{2+}$ solution with high concentration (2 mM) hemin (F).

was shown as A. And then, an increased ECL signal B was obtained by consuming the quencher O_2. Afterward, as the phenomenon we found, an enhanced signal was shown as C after adding hemin into pure $Ru(bpy)_3^{2+}$ solution. The possible explanation might be the interaction between low concentration (2.0 nM) hemin and dissolved O_2, which consumed the quencher. For the further exploration of the mechanism of hemin in $Ru(bpy)_3^{2+}$ solution, two control experiments were designed, ECL signal in $Ru(bpy)_3^{2+}$ solution which was added hemin after deoxygenating was shown as D. The ECL signal in $Ru(bpy)_3^{2+}$ solution which was deoxygenated after adding hemin was shown as E. It was obvious that after deoxygenating, the addition of hemin could not enhance the $Ru(bpy)_3^{2+}$ ECL signal. Moreover, after adding hemin, the deoxygenation could not enhance the $Ru(bpy)_3^{2+}$ ECL signal as well. There was a sharp contrast in the results of C, D and E. The ECL signal enhanced obviously in C due to the consumption of dissolved oxygen. And then, the ECL signal was suppressed in $Ru(bpy)_3^{2+}$ solution added with hemin after deoxygenating and in $Ru(bpy)_3^{2+}$ solution (D) added with hemin before deoxygenating (E), respectively. The phenomenon may be attributed to that once hemin does not react with dissolved oxygen, it can inhibit the ECL behavior of $Ru(bpy)_3^{2+}$. Finally, the ECL signal in $Ru(bpy)_3^{2+}$ solution with high concentration (2 mM) hemin was shown as F. The quenching effect might be attributed to the interaction of high concentration hemin with $Ru(bpy)_3^{2+}$ rather than with the quencher O_2.

To further verify the mechanism, the cyclic voltammetry (CV) experiments of six-group control were investigated as shown in the Supporting Information (SI) Figure S1. Compared with the standard $Ru(bpy)_3^{2+}$ solution (A), after deoxidation (B) or addition of low concentration hemin (C), the oxidation current increased obviously. The results demonstrated that removal or consumption of dissolved oxygen made the annihilation reaction of $Ru(bpy)_3^{2+}$ stronger, resulting in higher electron transfer. Moreover, two-group experiments with different order of hemin-addition and deoxidation were designed (D group and E group). The results showed that the $Ru(bpy)_3^{2+}$ oxidation current decreased, which was approximately the same as that in the group with high concentration of hemin (F group). These results demonstrate that the electron transfer became lower due to the inhibition of the annihilation reaction of $Ru(bpy)_3^{2+}$ by hemin. The results of CV were basically consistent with those of ECL.

3.2. The Characterization and Structure Optimization of DNA Nanotweezers. To confirm effective self-assembly process of the DNA nanotweezers, the hybridization reaction products were characterized by 2% agarose gel electrophoresis. As shown in SI Figure S2A, with the hybridization of A1, A2 and A3, the clear band exhibited the formation of the opened DNA nanotweezers (Lane 1). Moreover, after adding target into the reaction solution, the closed DNA nanotweezers were successfully constructed (Lane 2). On the contrary, the hybridization of A2 with A3 and A1 with A3 had a mobility corresponding to a 60−80 base pair marker (Lane 3 and 4), indicating that the functional DNA nanotweezers could not be constructed. Those results demonstrated the programmed assembly as expected. In addition, the CL results were listed (shown in SI Figure S2B) for further proving the formation of G4-hemin.

3.3. The Characterization of DNA−Ru(II)−Chitosan Film. Scanning electron microscope (SEM) was performed to prove the formation of DNA−Ru(II)−Chitosan film. SI Figure S3A illustrated the DNA−Ru(II) film with disperse-distributed small hole and rough surface, and the vision field was bright. In contrast, with the process of polymerization reaction between DNA and chitosan, the DNA−Ru(II)−Chitosan film (shown in SI Figure S3B) showed a sticky and smooth surface, and the field of vision was relatively dim. The difference of visual field brightness might be attributed to the decrease of electrical conductivity of biofilm when chitosan was added into biofilm. Finally, SI Figure S3C represented SEM of DNA−Ru(II)−Chitosan (high content) film by continuously adding chitosan. With the increase of the concentration of chitosan, the surface was viscous and massive. The difference of surface between the film with chitosan and without chitosan indicated that the DNA−Ru(II)−Chitosan film was successfully constructed.

3.4. DNA−Ru(II)−Chitosan Film Layer-by-Layer Fabrication with ECL Characterization Behaviors. ECL analyzer was used to monitor the interface properties of electrode during stepwise modifications in the voltage range from 0.5 to 1.25 V with 100 mV/s, and the voltage of the photomultiplier tube (PMT) was set at 700 V. It was observed that the bare Au electrode exhibited no ECL signal (Figure 2 curve a). Whereas after DNA film was assembled, there was none ECL signal as well (Figure 2 curve b). When Ru(II)−Chitosan mixture was dropped onto electrode modified by DNA film, the ECL signal increased (Figure 2 curve c). Subsequently, with addition of hemin, the closed DNA nanotweezers (with target) were added and adsorbed on the electrode by the electrostatic effect from chitosan, the ECL signal was as "OFF" signal and shown in Figure 2 curve d. However, when without target, the ECL signal enhanced largely (Figure 2 curve e). Furthermore, for reducing the nonspecific binding, a block ending was designed based on the condition of curve f, and the resulting ECL signal was as "ON" signal (Figure 2 curve f). Moreover, the EIS results of the formation progress of DNA−Ru(II)−Chitosan film were listed (shown in SI Figure S4). The results proved that the

DOI: 10.1021/acsami.8b18497
ACS Appl. Mater. Interfaces 2019, 11, 3715−3721

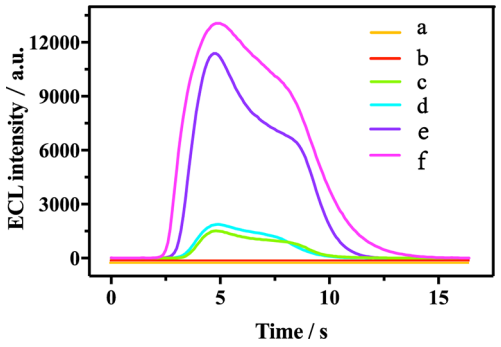

Figure 2. ECL responses of bare Au (a); Au modified by DNA film (b); Au modified by DNA−Ru(II)−Chitosan (c); Au modified by DNA−Ru(II)−Chitosan film with the absorption of closed DNA nanotweezer with hemin (d); Au modified by DNA−Ru(II)−Chitosan film with the absorption of opened DNA nanotweezer with hemin (e); Au modified by DNA−Ru(II)−Chitosan film with the absorption of opened and optimized DNA nanotweezer with hemin (f).

modification and reaction were as described in the principle Scheme 1.

3.5. Optimization of Experimental Conditions. Generally, when split functional domains are used in the development of complementation assays, it is essential to adjust the distal relationship of the split domains to reduce the background signal. Thus, the base-pair loop of spacer in A3 middle part was in the connecting part of recognized sites of A3 with A1 and A2. The number of base-pair was optimized by adding thymine ("T" base) in loop. As shown in SI Figure S5A, the lowest background ECL signal was about 3000 a.u at 4-base-pair. Therefore, 4-base-pair spacer as an optimal condition was applied in the following experiments. Moreover, for reducing the noise signal from nonspecific binding, 2-base pair block ending was designed on the connection of G-rich chain and nanotweezer arm, which would avoid the formation of G-4 without target (SI Figure S5B).

Furthermore, as the readout signal depended on the value of ON/OFF in this work, even though hemin provided an increasing signal in the absence of the target as the increase of hemin concentration. However, the quantity of hemin in solution can also influence the quenching effect by enhancing the "OFF" signal. Therefore, for investigating the highest ON/OFF, in the presence of target (400 pM), the concentration of hemin was optimized as shown in Figure 3A. At the hemin concentration of 2.0 nM, the resulting ON/OFF ratio was the highest. Thus, this concentration of hemin was selected as the optimal condition in subsequent experiments.

To maximize the efficiency of quenching, the formation time of closed nanotweezer (just the incubation time of hemin) in solution was also investigated in this work. As shown in SI Figure S6A, it was clear that the 45 min incubation obtained the lowest signal due to the quenching effect of the closed nanotweezer. Thus, 45 min was chosen as the optimal time of hemin incubation.

To enhance the stability of ECL signal, the ratio of $Ru(bpy)_3^{2+}$ to chitosan (R/C) in DNA−Ru(II)−Chitosan film and the incubation time of DNA−Ru(II)−Chitosan film were also optimized (shown in Figure 3B and SI Figure S6B). In the optimization of the ratio with a stable concentration of $Ru(bpy)_3^{2+}$, as the ratio of R/C decreased, the signal stability increased, and the slope value closed to 1 (k value). Therefore, the signal in the ratio of 5:4 (R/C) was chosen for the next-step experiment (shown in Figure 3B). Additionally, the ECL signal improved rapidly as the incensement of the incubation time, and eventually stabilized when the incubation time was over 20 min. Thus, 20 min was selected as an optimal incubation time of hemin in the following experiments.

3.6. Analytical Performance of the Biosensing Strategy. To assess the analytical performance of the proposed biosensor, the DNA nanotweezers were incubated with different concentrations of PML/RARα under the optimized conditions. As shown in Figure 4A and, the ECL intensity decreased correspondingly with the concentration of the target PML/RARα in the range of 1 fM to 1 nM. The linear regression equation was "$Y = -1394 \times \lg C_{PML/RAR\alpha} - 1734$" with a squared correlation coefficient of 0.9944 (Figure 4B), and the limit of detection was estimated to be 0.125 fM (LOD, defined as 3σ of the signal from the blank). Compared with the reported biosensors (shown in SI Table S2), the developed biosensor showed a wider linear range and a lower detection limit due to the excellent ECL signal enhancement effect of low concentration hemin controlled by nanotweezer.

3.7. Specificity, Stability and Repeatability for PML/RARα Detection. To investigate the specificity of the proposed biosensor, the ECL response signal of "L" subtype PML/RARα was compared with that of single PML DNA, single RARα DNA, and PML/RARα DNA in different subtypes ("S" and "V" subtypes) in Figure 5A. Surprisingly, no obvious ECL signal decrease could be observed in the detection of PML, RARα, "S" type, and "V" type as compared with that in target. Therefore, these results indicated that the developed biosensor manifested good specificity.

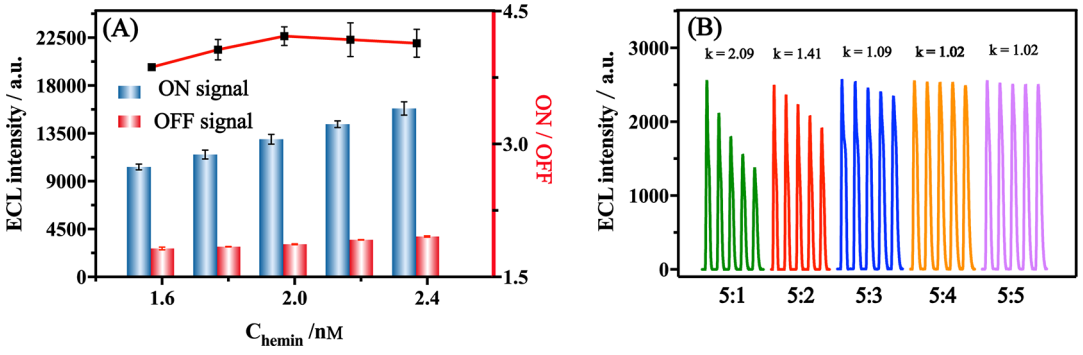

Figure 3. (A) Optimization of hemin concentration for the most ON/OFF (the ratio of "ON" signal to "OFF" signal) (B) ECL intensity of the biosensor on different ratio of Ru(II)/Chitosan in DNA−Ru(II)−Chitosan film (5:1, 5:2, 5:3, 5:4, 5:5).

DOI: 10.1021/acsami.8b18497
ACS Appl. Mater. Interfaces 2019, 11, 3715−3721

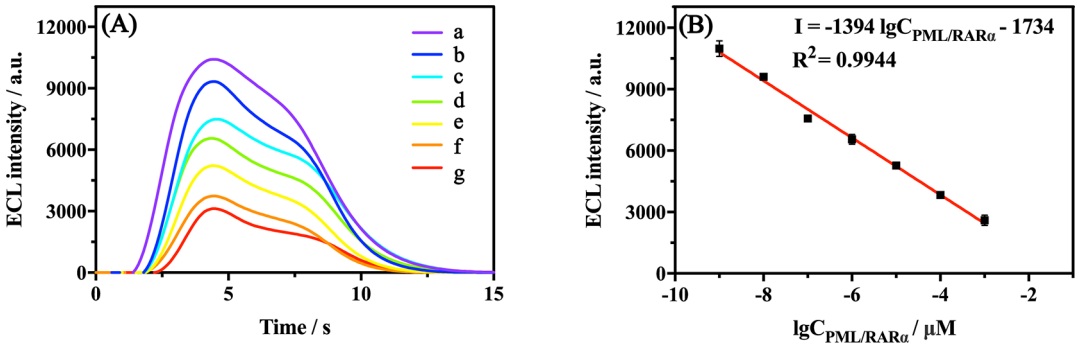

Figure 4. (A) Relationship between the change of ECL intensity and the logarithm of the concentration of PML/RARα. (B) ECL intensity-time curves of the biosensor with different concentrations of PML/RARα in 0.1 M PBS (pH 7.4) containing 0.1 mM KCL. PML/RARα concentrations: (a) 1 fM; (b) 10 fM; (c) 0.1 pM; (d) 1 pM; (e) 10 pM; (f) 0.1 nM; (g) 1 nM.

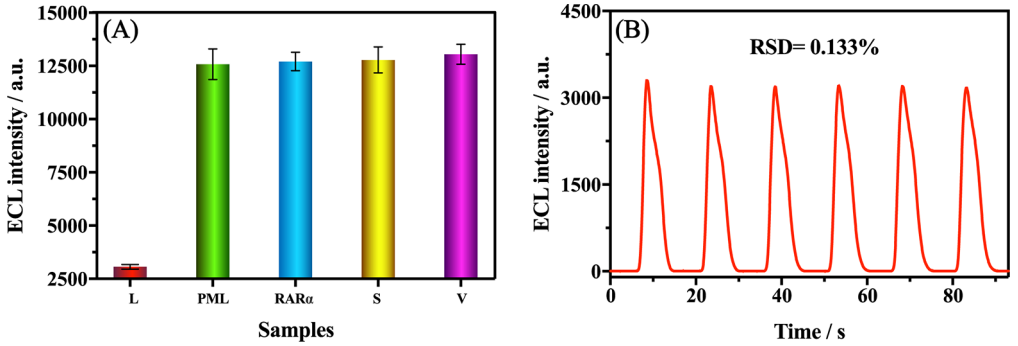

Figure 5. (A) ECL response signals for specificity of PML/RARα detection against PML/RARα DNA "L" subtype (target) and different nontargets: PML DNA, RARα DNA, PML/RARα DNA "S" subtype, PML/RARα DNA "V" subtype. Error bar represents the standard deviation (n = 3). (B) The stability of the ECL system in six cycles.

The stability of the biosensor was of great significance for adapting to the long testing processes. Six cycles of the continuous ECL scan were monitored to study the stability of the biosensor in 0.1 M PBS (pH 7.4). As shown in Figure 5B, no obvious fluctuation (RSD = 0.133%) was observed with the ECL peak intensity during continuous scanning, indicating favorable stability of the proposed biosensor.

The repeatability of the method was investigated by analyzing five different concentrations prepared under the same condition (shown in SI Table S3), with PML/RARα fusion gene as model target, and an average coefficient of variation (CV) of 1.57 was obtained. The results indicated that the designed method for PML/RARα fusion gene detection exhibited an acceptable repeatability.

3.8. Standard Recovery Test of the Biosensor in Salmon Sperm Sample. To assess the reliability of the developed method in complex biological mechanism, the recovery tests were performed by using salmon sperm DNA, shown in SI Table S4. Samples of three different concentrations were prepared by mixing synthetic PML/RARα DNA with 10 mg/mL salmon sperm DNA. The recoveries were 102.54%, 96.15%, and 103.69% in concentrations of 10 fM, 1 pM, and 100 pM, respectively, indicating that the developed method was a feasible approach for target DNA analysis in complex biological sample.

4. CONCLUSION

In this work, low concentration of hemin was first proved as the $Ru(bpy)_3^{2+}$ ECL enhancer by consuming quencher O_2 in $Ru(bpy)_3^{2+}$ ECL system. Based on this discovery, an enzyme-free and pragmatic ECL biosensor was successfully developed for quantitative analysis of PML/RARα with target-switched DNA nanotweezer and stable DNA–Ru(II)–Chitosan film. The developed biosensor exhibited target-depended "ON-OFF" switching with high flexibility due to the signal enhancement from the consumption of quencher O_2 and quenching effect after the formation of closed nanotweezer. In addition, compared with the reported fusion gene detection strategy, this developed method by one-step reaction for PML/RARα detection possessed a wider detection range and lower detection limit, which might provide a promising alternative tool for the detection of fusion gene in the future.

■ ASSOCIATED CONTENT

Supporting Information

The Supporting Information is available free of charge on the ACS Publications website at DOI: 10.1021/acsami.8b18497.

Tables for oligonucleotides sequences, comparison among analytical performances, reproducibility of sensing method, recovery results, figures for agarose gel electrophoretic analysis, CL results of G4-hemin formation, SEM results of biofilm. EIS results of layer-by-layer on the electrode, condition optimization (PDF)

■ AUTHOR INFORMATION

Corresponding Author

*(S.J.D.) Phone: +86-23-68485688; fx: +86-23-68485786; e-mail: dingshijia@163.com and dingshijia@cqmu.edu.cn.

ORCID

Wei Cheng: 0000-0002-1921-9761

DOI: 10.1021/acsami.8b18497
ACS Appl. Mater. Interfaces 2019, 11, 3715–3721

Shijia Ding: 0000-0002-9183-1656

Author Contributions

[‖]X.B. and B.G. contributed equally to this work.

Notes

The authors declare no competing financial interest.

■ ACKNOWLEDGMENTS

This research was supported by the National Natural Science Foundation of China (81873980 and 21804015), the Natural Science Foundation Project of CQ CSTC (cstc2018jcyjAX0206) and the Special Project for Social Livelihood and Technological Innovation of Chongqing (cstc2016shmszx130043).

■ REFERENCES

(1) Xu, X. W.; Wang, L.; Li, K.; Huang, Q. H.; Jiang, W. A smart DNA Tweezer for Detection of Human Telomerase Activity. *Anal. Chem.* **2018**, *90*, 3521−3530.

(2) Zadegan, R. M.; Jepsen, M. D.; Thomsen, K. E.; Okholm, A. H.; Schaffert, D. H.; Andersen, E. S.; Birkedal, V.; Kjems, J. Construction of a 4 Zeptoliters Switchable 3D DNA Box Origami. *ACS Nano* **2012**, *6*, 10050−10053.

(3) Bradley, C. A. DNA nanorobots - seek and destroy. *Nat. Rev. Drug Discovery* **2018**, *18*, 242.

(4) Guo, B.; Cheng, W.; Xu, Y. J.; Zhou, X. Y.; Li, X. M.; Ding, X. J.; Ding, S. J. A simple Surface Plasmon Resonance Biosensor for Detection of PML/RARα based on Heterogeneous Fusion gene-triggered Nonlinear Hybridization Chain Reaction. *Sci. Rep.* **2017**, *7*, 14037.

(5) Zhou, X. Y.; Zhao, M.; Duan, X. L.; Guo, B.; Cheng, W.; Ding, S. J.; Ju, H. X. Collapse of DNA Tetrahedron Nanostructure for "Off-On" Fluorescence Detection of DNA Methyltransferase activity. *ACS Appl. Mater. Interfaces* **2017**, *9*, 40087−40093.

(6) Tian, T.; Li, J.; Xie, C.; Sun, Y. H.; Lei, H. Z.; Liu, X. Y.; Xia, J. Y.; Shi, J. Y.; Wang, L. H.; Lu, W. Y.; Fan, C. H. Targeted Imaging of Brain tumors with a Framework Nucleic Acid Probe. *ACS Appl. Mater. Interfaces* **2018**, *10*, 3414−3420.

(7) Jiang, D. W.; Sun, Y. H.; Li, J.; Li, Q.; Lv, M.; Zhu, B.; Tian, T.; Cheng, D. F.; Xia, J. Y.; Zhang, L.; Wang, L. H.; Huang, Q.; Shi, J. Y.; Fan, C. H. Multiple-armed Tetrahedral DNA Nanostructures for Tumor-targeting, Dual-modality in Vivo imaging. *ACS Appl. Mater. Interfaces* **2016**, *8*, 4378−4384.

(8) Guo, B.; Wen, B.; Cheng, W.; Zhou, X. Y.; Duan, X. L.; Zhao, M.; Xia, Q. F.; Ding, S. J. An Enzyme-free and Label-free Surface Plasmon Resonance biosensor for ultrasensitive Detection of Fusion gene based on DNA Self-assembly Hydrogel with Streptavidin Encapsulation. *Biosens. Bioelectron.* **2018**, *112*, 120−126.

(9) He, L.; Lu, D. Q.; Liang, H.; Xie, S.; Luo, C.; Hu, M.; Xu, L.; Zhang, X.; Tan, W. Fluorescence Resonance Energy Transfer-based DNA Tetrahedron Nanotweezer for highly reliable Detection of Tumor-related mRNA in Living cells. *ACS Nano* **2017**, *11*, 4060−4066.

(10) Li, D. D.; Cheng, W.; Li, Y. J.; Xu, Y. J.; Li, X. M.; Yin, Y. B.; Ju, H. X.; Ding, S. J. Catalytic Hairpin Assembly actuated DNA Nanotweezer for Logic gate building and sensitive Enzyme-free biosensing of MicroRNAs. *Anal. Chem.* **2016**, *88*, 7500−7506.

(11) Dong, Y. P.; Wang, J.; Peng, Y.; Zhu, J. J. A novel Aptasensor for Lysozyme based on Electrogenerated Chemiluminescence Resonance Energy Transfer between luminol and silicon quantum dots. *Biosens. Bioelectron.* **2017**, *94*, 530−535.

(12) Chang, M. M.; Saji, T.; Bard, A. J. Electrogenerated Chemiluminescence. 30. electrochemical oxidation of oxalate ion in the presence of Luminescers in Acetonitrile solutions. *J. Am. Chem. Soc.* **1977**, *8*, 5399−5403.

(13) Fa ¨hnrich, K. A.; Pravda, M.; Guilbault, G. G. Recent applications of Electrogenerated Chemiluminescence in Chemical Analysis. *Talanta* **2001**, *54*, 531−559.

(14) Zhai, Q. F.; Li, J.; Wang, E. K. Recent advances based on Nanomaterials as Electrochemiluminescence Probes for the Fabrication of sensors. *ChemElectroChem* **2017**, *4*, 1639−1650.

(15) Richter, M. M. Electrochemiluminescence (ECL). *Chem. Rev.* **2004**, *104*, 3003−3036.

(16) Xing, H. H.; Zhai, Q. F.; Zhang, X. W.; Li, J.; Wang, E. K. Boron Nitride quantum dots as efficient Coreactant for enhanced Electrochemiluminescence of Ruthenium(II) tris(2,2′-bipyridyl). *Anal. Chem.* **2018**, *90*, 2141−2147.

(17) Joseph, I.; Cline, III.; Walter, J. D.; James, N. D.; Benjamin, A. deGraff. .beta.-Cyclodextrin inclusion Complexes with. alpha. -Diimine Ruthenium(II) Photosensitizers. *J. Phys. Chem.* **1985**, *89*, 94−97.

(18) Zhao, M.; Liao, N.; Zhuo, Y.; Chai, Y. Q.; Wang, J. P.; Yuan, R. Triple Quenching of a novel Self-enhanced Ru(II) Complex by Hemin/G-quadruplex DNAzymes and its potential Application to Quantitative protein detection. *Anal. Chem.* **2015**, *87*, 7602−7609.

(19) Li, H.; Chen, J.; Han, S.; Niu, W.; Liu, X.; Xu, G. Electrochemiluminescence from Tris(2,2′-bipyridyl) Ruthenium(II)-Graphene-nafion modified electrode. *Talanta* **2009**, *79*, 165−170.

(20) Tsuneyasu, S.; Takahashi, R.; Minami, H.; Nakamura, K.; Kobayashi, N. Ultrafast Response in AC-driven Electrochemiluminescent Cell using Electrochemically active DNA/$Ru(bpy)_3^{2+}$ Hybrid film with Mesoscopic structures. *Sci. Rep.* **2017**, *7*, 8525.

(21) Jirka, G. P.; Nieman, T. A. Modulated potential Electrogenerated Chemiluminescence of Luminol and $Ru(bpy)_3^{2+}$. *Microchim. Acta* **1994**, *113*, 339−347.

(22) Matheu, R.; Moreno-Hernandez, I. A.; Sala, X.; Gray, H. B.; Brunschwig, B. S.; Llobet, A.; Lewis, N. S. Photoelectrochemical Behavior of a Molecular Ru-based Water-Oxidation Catalyst Bound to TiO_2-protected Si Photoanodes. *J. Am. Chem. Soc.* **2017**, *139*, 11345−11348.

(23) Ma, H. M.; Li, X. J.; Yan, T.; Li, Y.; Liu, H. Y.; Zhang, Y.; Wu, D.; Du, B.; Wei, Q. Sensitive Insulin Detection based on Electrogenerated Chemiluminescence Resonance Energy Transfer between $Ru(bpy)_3^{2+}$ and Au nanoparticle-doped β-cyclodextrin-Pb(II) Metal-Organic Framework. *ACS Appl. Mater. Interfaces* **2016**, *8*, 10121−10127.

(24) Du, Y.; Qi, B.; Yang, X. R.; Wang, E. K. Synthesis of PtNPs/AQ/$Ru(bpy)_3^{2+}$ Colloid and its Application as a sensitive Solid-state Electrochemiluminescence Sensor material. *J. Phys. Chem. B* **2006**, *110*, 21662−21666.

(25) Sacco, P.; Brun, F.; Donati, I.; Porrelli, D.; Paoletti, S.; Turco, G. On the Correlation between the Microscopic structure and properties of Phosphate-Cross-Linked chitosan gels. *ACS Appl. Mater. Interfaces* **2018**, *10*, 10761−10770.

(26) Yang, Y. M.; Guo, M.; Qian, R.; Liu, C.; Zong, X. M.; Li, Y. Q.; Li, W. F. Binding Efficacy and Kinetics of chitosan with DNA duplex: The effects of Deacetylation Degree and Nucleotide Sequences. *Carbohydr. Polym.* **2017**, *169*, 451−457.

(27) Hagan, K. A.; Meier, W. L.; Ferrance, J. P.; Landers, J. P. Chitosan-coated Silica as a solid phase for RNA Purification in a Microfluidic Device. *Anal. Chem.* **2009**, *81*, 5249−5256.

(28) Dang, J.; Guo, Z.; Zheng, X. Label-free sensitive Electrogenerated Chemiluminescence Aptasensing based on Chitosan/$Ru(bpy)_3^{2+}$/silica Nanoparticles Modified Electrode. *Anal. Chem.* **2014**, *86*, 8943−8950.

(29) Steckl, A. J. DNA - A New Material for Photonics? *Nat. Photonics* **2007**, *1*, 3−5.

(30) Goddard, A. D.; Borrow, J.; Freemont, P. S.; Solomon, E. Characterization of a Zinc finger gene Disrupted by the t (15;17) in Acute Promyelocytic Leukemia. *Science* **1991**, *254*, 1371−1374.

(31) Ito, K.; Bernardi, R.; Morotti, A.; Matsuoka, S.; Saglio, G.; Ikeda, Y. PML Targeting Eradicates Quiescent Leukaemia-Initiating Cells. *Nature* **2008**, *453*, 1072−1078.

DOI: 10.1021/acsami.8b18497
ACS Appl. Mater. Interfaces 2019, 11, 3715−3721